fNIRS-EEG study of focal interictal epileptiform discharges

Running title: fNIRS-EEG study of IEDs

Ke Peng[a], Dang Khoa Nguyen[b], Tania Tayah[b], Phetsamone Vannasing[c], Julie Tremblay[c], Mohamad Sawan[a], Maryse Lassonde[c,d], Frédéric Lesage[a,e], Philippe Pouliot[a,e,*]

[a]*Département de génie électrique, École Polytechnique de Montréal, C.P.6079, Succ. Centre-ville, Montréal, Qc, Canada H3C3A7*

[b]*Service de neurologie, Hôpital Notre-Dame du CHUM, 1560 Rue Sherbrooke Est, Montréal, Qc, Canada H3L4M1*

[c]*Centre de recherche, Hôpital Sainte-Justine, 3175 Chemin de la côte-Sainte-Catherine, Montréal, Qc, Canada H3T1C5*

[d]*Centre de recherche en neuropsychologie et cognition, Département de psychologie, Université de Montréal, Montréal, Qc, Canada H3C3J7*

[e]*Institut de cardiologie de Montréal, Centre de recherche, 5000 Rue Bélanger Est, Montréal, Qc, Canada H1T1C8*

Abstract

Functional near-infrared spectroscopy (fNIRS) acquired with electroencephalography (EEG) is a relatively new non-invasive neuroimaging technique with potential for long term monitoring of the epileptic brain. Simultaneous EEG-fNIRS recording allows the spatio-temporal reconstruction of the hemodynamic response in terms of the concentration changes in oxy-hemoglobin (HbO) and deoxy-hemoglobin (HbR) associated with recorded epileptic events such as interictal epileptic discharges (IEDs) or seizures. While most previous studies investigating fNIRS in epilepsy had limitations due to restricted spatial coverage and small sample sizes, this work includes a sufficiently large number of channels to provide an extensive bilateral coverage of the surface of the brain for a sample size of 40 patients with focal epilepsies. Topographic maps of significant activations due to each IED type were generated in four different views (dorsal, frontal, left and right) and were compared with the epileptic focus previously identified by an epileptologist.

After excluding 5 patients due to the absence of IEDs and 6 more with mesial temporal foci too deep for fNIRS, we report that significant HbR (respectively HbO) concentration changes corresponding to IEDs were observed in 62% (resp. 38%) of patients with neocortical epilepsies. This HbR/HbO response was most significant in the epileptic focus region among all the activations in 28%/21% of patients.

Keywords:

Focal epilepsy, fNIRS, NIRS-SPM, EEG, interictal epileptic discharges

[*] Corresponding author; Tel.: +1-514-340-4711x2306; fax: +1-514-340-4611; e-mail: ph.pouliot@gmail.com

Abstract: 209 words

Text: 4541 words

Numbers of references: 37

Number of text pages: 11

Number of tables: 2

Number of figures: 2

Supplementary data: 2 tables

All authors report no disclosures.

The study is not industry-sponsored.

Introduction

Functional near-infrared spectroscopy (fNIRS) is a promising functional imaging approach to monitor brain activity (Jöbsis, 1977). Since hemoglobin is the main absorber of near-infrared (NIR) light (wavelengths in the range from 650 nm to 900 nm), fNIRS is capable of recording the concentration changes in deoxy-hemoglobin (HbR), oxy-hemoglobin (HbO) and total hemoglobin (HbT, which is a proxy for regional cerebral blood volume (rCBV)) in the human brain using their spectroscopic properties (Delpy and Cope, 1997; Desjardins et al., 2012). Application of fNIRS to epilepsy research is of interest as it offers the potential for long-term non-invasive and high temporal resolution hemodynamic imaging, with perhaps more flexibility in experimental setup including lower cost and portability (Irani et al., 2007; Lloyd-Fox et al., 2010; Lareau et al., 2011). With electroencephalographic (EEG) signals simultaneously acquired with fNIRS, the hemodynamic changes associated with epileptiform events such as interictal epileptiform discharges (IEDs) and seizures can be investigated. Using a high number of channels for extended spatial coverage, our group has recently shown the potential of fNIRS to accurately detect hemodynamic changes associated with focal seizures, localize the epileptic focus and characterize the complex local and remote oxygenation changes occurring during such events (Nguyen et al., 2012, 2013). However, because seizures are random and seldom occur during EEG-fNIRS testing, we sought to determine if IEDs captured during these long recordings could also provide useful localization information, as IEDs have been shown to be highly correlated with seizures and are also considered as fundamental components contributing to epileptogenesis (Staley and Dudek, 2006; Gotman et al., 2006; Gotman, 2008).

Although IEDs are more easily captured during recordings than seizures and generally not associated with movement artifacts, they are associated with a weaker neurovascular response than seizures, which poses additional methodological challenges. In a preliminary investigation, we previously showed the feasibility of recording the hemodynamic response due to IEDs with

EEG-fNIRS (Machado et al., 2011). There we found a spatially concordant increase in rCBV at the epileptogenic focus on one patient with focal epilepsy, and on three more in Pouliot et al. (2012) where concordance with EEG-fMRI was investigated. Here, we extend the results of this work to a larger dataset of forty patients. Our main objectives are to investigate the distribution of activations associated with IEDs and to evaluate the preclinical value of using only EEG-fNIRS data for focus localization.

Methods

Simultaneous EEG-fNIRS recording

Forty patients with refractory focal epilepsy investigated for potential epilepsy surgery underwent continuous EEG-fNIRS recording at the Optical Imaging Laboratory of Saint-Justine Hospital. The study was approved by the Ethics Committees of Sainte-Justine and Notre-Dame Hospitals and informed consents were obtained from all subjects. Most EEG-fNIRS studies were performed while patients were admitted for video-EEG monitoring as part of their presurgical evaluation, at which time anticonvulsants were frequently reduced or tapered for clinical purposes. An epileptologist was available at all times to ensure patient safety. In addition to video-EEG monitoring, the comprehensive presurgical evaluation included ictal single photon computed tomography (iSPECT), positron emission tomography (PET), anatomical brain magnetic resonance imaging (MRI) and magnetoencephalography (MEG). When needed, an intracranial EEG study was performed. Localization of the most plausible epileptic focus region was carried out by an epileptologist (DKN), following standard methodology as is done in major epilepsy centers: by looking for congruency among the results of clinical semiology analysis, location of scalp interictal and ictal EEG findings, location of the epileptogenic lesion on MRI when present, activations during iSPECT, source localizations by MEG, findings from intracranial EEG recordings when available, etc. The epicenter of the epileptic focus was then transposed onto the 3D brain. The extent of the epileptic focus was arbitrarily set as a 30mm radius sphere around this epicenter.

A detailed description of the EEG-fNIRS recording process can be found in Nguyen et al. (2012). Briefly, custom helmets for different head sizes were designed to mount 64 fibered light sources and up to 16 detectors, as well as 19 carbon EEG electrodes onto the patient heads. For each patient, optode and electrode positions were co-registered onto a 3-D high resolution anatomical MRI image (obtained previously) using the BrainSight software (Rogue-Research, Montreal, Canada). The EEG was recorded at 500Hz with a Neuroscan Synamps 2TM system (Compumedics, USA). A band-pass filter between 0.1Hz and 100Hz was applied to remove instrumental noise and other artificial disturbances. The fNIRS data was captured simultaneously using a multi-channel *Imagent* Tissue Oximeter (ISS Inc., Champaign, IL, USA). The oximeter employed a frequency-domain method which implied that light sources are intensity modulated over time at 110MHz. Optical channels, consisting of one fiber source and one detector that could see several sources, were usually three to five centimetres apart to ensure sensitivity to

cortical tissue. Two different wavelengths were used in recordings, one at 690nm which is more sensitive to HbR and the other one at 830nm which is more sensitive to HbO, and were both recorded through multiple optical channels (115±39 channels per subject). The channel positions were intentionally arranged so that the covered area would include the whole lobe that contained the most probable epileptic focus, the contralateral lobe, and as much area as possible of the other lobes. The DC light intensity probed by detectors was sampled at a frequency of 19.5Hz. Two to twelve sessions (sometimes called "runs" in the fMRI literature) of typically 15 minutes each were recorded for each patient. During the recordings, the patient was simply asked to sit comfortably in a chair and relax. IED regressors and possible seizure regressors were marked offline on the EEG trace using Analyzer 2.0 (Brain Products GmbH, Germany) by a certified clinical neurophysiologist (TT) and reviewed by an epileptologist (DKN). For the 12 patients who had more than one type of IEDs, these were divided in distinct IED types (e.g.1. right temporal spikes and left temporal spikes in some patients with bi-temporal lobe epilepsy; e.g.2. right frontal spikes and diffuse spike and wave from secondary bilateral synchrony in some other patients). IEDs of each type were only analyzed if they occurred frequently enough (>1/200 Hz, i.e. at least 18 IEDs per hour). From the recorded electrocardiogram, a heartbeat rate regressor was derived and manually checked to correct inaccuracies.

Data processing

The fNIRS data was processed with a Matlab (MathWorks, USA) toolbox developed in-house, called nirs10 (available upon request), based on SPM8 (Friston et al., 2007) and NIRS-SPM (Ye et al., 2009; Jang et al., 2009). Channels with source-detector separation greater than 6 cm or with standard deviation greater than 10% of the mean were removed right away and were not included in channel counts presented later on, following (Nguyen et al., 2012, 2013). Concentration changes of HbR and HbO were obtained from light intensity using the modified Beer-Lambert Law. Principal component analysis (PCA) was performed on NIRS data and, following data inspection, one component with the most variance was removed, to reduce movement such as sudden jumps affecting most channels as well as other artifacts such as large physiological responses, common to all channels, and presumed unrelated to the IED response. Concentration changes were then high-pass filtered with an infinite response 4^{th} order Butterworth filter at 0.01Hz, and low-pass filtered using a filter with the shape of the canonical SPM8 hemodynamic response function (HRF).

The hemoglobin concentration changes Y for each channel were fitted by a general linear model (GLM), namely a decomposition of the response variable Y into a linear combination of explanatory variables X_i plus an error term ε, $Y = X\beta + \varepsilon$. The design matrix X contained one regressor for each IED type, and several additional confound regressors included only as confounds, i.e. to remove variance in the data, and not further studied in this work: regressors for all seizure-like events, a heart rate regressor and a constant. The IEDs were treated as brief impulsions of equal amplitude and their contribution to the design matrix was calculated by

convolving their timing with a canonical HRF (Friston et al., 1998). The pre-coloring method (Ye et al., 2009) was used to add known correlated noise, as in Pouliot et al. (2012) .

Coregistration and contrasts

For each patient, an anatomical MRI was segmented into six different layers (air, scalp, skull, CSF, grey matter and white matter). The grey matter layer was used to extract six two-dimensional cortical projections. The three-dimensional position of each channel was projected onto these two-dimensional topographic maps, of which 4 views were considered: dorsal, frontal, left and right views. Two-dimensional contrast maps for each IED type were finally generated by interpolation of the amplitudes, β_i, of the hemodynamic responses for the four views, as well as for each session of each patient. Patient-level analysis followed the analysis of each session as a way to pool the information from all the recorded sessions. As in Ye et al., 2009, this was done by a precision-weighted average of the session contrast maps.

There is evidence that during IEDs a compensatory increase in rCBV in the focus region could be expected, concomitantly with a decrease in local HbR and an increase in local HbO and HbT, to provide extra oxygen supply to the epileptic tissue (Penfield and Jasper, 1954; Saito et al., 1995; Suh et al., 2006; Geneslaw et al., 2011). Thus at each location on 2D maps, a hemodynamic response to IEDs was called "standard", or non-inverted, if the response at that location was a negative change for HbR, or a positive change for HbO/HbT.

One-tailed *t*-statistic maps (T-maps) were obtained for each IED type, testing the null hypothesis that the HbR did not decrease (resp. that HbO or HbT did not increase), with the other IED types considered as potential confounds.

Assuming a *p*-value of 0.05, the patient-level significance of the hemodynamic responses to IEDs was decided upon a peak False Discovery Rate (pFDR) correction. A rigorous implementation of pFDR for NIRS is beyond the scope of this paper. Instead, the following heuristic procedure was used (denoted as 2D-pFDR): 1- a list was made of the uncorrected p-values of the pixels at the local peaks on the 2D contrast map of the view of interest. This view (usually left or right, sometimes dorsal) was chosen to best cover the location of the most frequent IED type. 2- Only those peaks which surpassed a first height threshold were then sent to the FDR-BH algorithm (Benjamini and Hochberg, 1995), where their p-values were treated as coming from independent tests. Here we chose u>2.5 as this first threshold as in Chumbley et al. (2010). This procedure produced a new height threshold which was then applied to the whole 2D T-maps of all the views to finally control the false positive rate of all pixels.

Sensitivity & specificity definition

The most plausible epileptic focus region, which was represented as a 30mm radius sphere around the epicenter of each patient, was also projected onto the four 2D views. The overlap between the projected focus and the patient-level statistical maps of activations could thus be assessed. The sensitivity and specificity, calculated separately on HbR maps or on HbO/HbT maps, were defined as follows: For each patient, a positive was decided for sensitivity if the

epileptic focus region overlapped a non-inverted significant "standard" hemodynamic response. A positive was decided for specificity if the change in HbR/HbO in the epileptic focus region was the most significant among the other significant HbR/HbO clusters, and thus would lead to a successful identification of the epileptic focus region. An observed hemoglobin concentration change was said to be the most significant if it occupied a larger area on the cortex than any other standard response all over the brain, or if it contained a higher maximum statistical score in case the areas of two or more clusters were very close in size. Specificity was set to negative if sensitivity was negative.

Results

Forty patients with drug-resistant epilepsy underwent an EEG-fNIRS study (26 males; mean age 33; range 10-62). Three of the forty patients (#19, #22, #34) were excluded as very few IEDs were detected on EEG recordings (#22, #34: no IED was captured; #19: only 1 IED was captured during a 15-minute recording); another (#17) was excluded because fNIRS optodes were not covering the epileptic focus due to technical problems, a fifth one (#37) was excluded because focus localization was clinically uncertain despite extensive multimodal evaluation. Subsequent data analysis was undertaken on the remaining 35 patients.

Table 1 provides the type and total number of IEDs that were recorded for each patient. According to conventional anatomy, each hemisphere of the brain was divided into four major lobes: Frontal (F), Temporal (T), Parietal (P) and Occipital lobes (O). Among the 35 remaining patients, 29 patients (83%) suffered from neocortical epilepsy while 6 patients had a mesial temporal focus.

--TABLE 1 NEAR HERE --

Because EEG-fNIRS can only sample the superficial cortex, data was examined separately between patients with neocortical epilepsies and mesial temporal lobe epilepsies (MTLE). For neocortical epilepsy, the markings of significant ($p<0.05$, 2D-pFDR corrected) concentration changes in HbR are depicted in Table 2, while the markings for HbO and HbT can be found in Appendix A. For MTLE, the results for all the chromophores are provided in Appendix B. In these tables, an up arrow ↑ (down arrow ↓) indicates that an increase (resp. a decrease) in the concentration of the hemoglobin was observed in the corresponding locations of the contrast maps. A double arrow sign ↑↑ or ↓↓ means that the given activation was recognised as being the most significant.

1. EEG-fNIRS response in neocortical epilepsies versus mesial temporal lobe epilepsies

1.A. Neocortical epilepsies

Detailed results from Patient #36 and Patient #7 are presented below to illustrate the analytical procedure, followed by a summary of results from all the 29 patients with a neocortical focus.

• Illustrative case 1 (Patient #36):

This 36 year-old man with pharmacoresistant predominantly nocturnal seizures had an epileptic focus in the left inferior frontal gyrus confirmed by MEG (Fig. 1(A)), intracranial EEG and a good surgical outcome following epilepsy surgery (Engel II; follow-up 3 years). 144 fNIRS and 19 EEG channels provided a full coverage of bilateral frontal lobe, temporal lobe and central areas (Fig.1(B)). Three types of IEDs were identified from four sessions with a total recording time of 50 min (Fig.2(C)): 1088 left fronto-temporal IEDs at a rate of 22 per minute (referred as type I IEDs); 1450 bi-frontal (L>R) IEDs at a rate of 29 per minute (type II); 5 left frontal IEDs at a rate of 6 per hour (type III). Ignoring type III IEDs due to their low frequency, we show the projection onto the grey matter image of 2D-pFDR corrected patient-level HbR concentration contrasts associated with type I and II IEDs in Fig.2(D) and (E). No significant HbO or HbT response to type I or type II IEDs was observed. The most probable epileptic focus region determined from pre-surgical evaluation was represented as a green circle of 30mm radius. Sensitivity and specificity were decided by jointly looking at the T-maps of type I and II IEDs: type I IEDs were ignored since only very small activations were present in the left and right pre-central gyrus. For type II IEDs, significant HbR decreases were located in the left inferior frontal gyrus and part of the left superior temporal gyrus, mostly inside the focus circle with a minimum t-value of -3.2. On the contralateral right inferior frontal gyrus, less significant HbR decreases were also located as expected with a minimum t-value of -2.9. Hence, both the sensitivity and the specificity were declared positive on HbR.

--FIGURE 1 NEAR HERE --

Comparing the T-maps of the left and the right view, experts could easily lateralize to the left hemisphere. A left inferior frontal focus could be immediately inferred for this patient, following the position of the most significant HbR decreases.

• Illustrative case 2 (Patient #7):

This 22-year-old man with pharmacoresistant gelastic seizures had an epileptic focus located in the right inferior frontal gyrus confirmed by MEG (Fig. 2(A)), intracranial EEG and seizure-freedom following epilepsy surgery (follow-up 1 year). Prior to surgery, three 15-minute sessions were recorded with EEG-fNIRS followed by a fourth session of 8.4 minutes. 134 NIRS channels (Fig.2(B)) were widely and symmetrically distributed on the helmet, providing a full coverage of the focus region as well as other lobes on the same right side or on the contralateral side. Fig. 2(C) shows a segment of EEG recording in Session 2 with 4 IEDs marked. A total number of 2302 right fronto-temporal IEDs were captured in the primary focus region, occurring at an overall rate of 43 per minute. In the meantime, 21 bi-frontal IEDs were also marked, arising at a rate of 23 per hour. Only the hemodynamic response to the right frontal-temporal IEDs is presented as the bi-frontal IEDs arose at less frequently than 1/200 Hz (actual analysis showed no significant activation). In Fig.2(D), T-maps from the patient-level one-tailed t-tests are depicted. T-thresholds from a 2D-pFDR correction procedure are calculated and applied for the contrast maps. The most plausible epileptic focus region was shown as a circle of 30mm radius.

--FIGURE 2 NEAR HERE --

The activated area in the right inferior frontal gyrus seen in Fig.2(D) was in good concordance with the focus region. A negative concentration change in HbR with a minimum t-value of -2.5, as well as positive changes in HbO and in HbT (resp. 3.5/3.4 maximal t-values), was observed in the green circle which describes the focus region, and was recognized as possible response to IEDs. On the contralateral side, homologous responses (decrease in HbR together with increases in HbO and in HbT) were found both inside and outside the dotted green circle. However, the contralateral response clusters seemed to be more scattered.

Although the analysis has shown sensitivity to the location of epileptic focus, stronger activations in the left superior frontal gyrus were present. Hence, current results with EEG-fNIRS for this patient do not allow specific identification of the focus.

• Summary of neocortical epilepsies (29 patients)

Among the 29 patients who had a neocortical focus, 18 patients (62%) had significant negative HbR concentration changes in the epileptic focus region, which led to a sensitivity of 62% for EEG-fNIRS in HbR. 8 patients (28% of 29 patients, 44% of the 18 patients whose sensitivity has been decided to be positive) had the most significant decrease in HbR in the focus region. Hence for our sample of patients with neocortical epilepsy, specificity of HbR measured was thus estimated to be 28%.

The results based on HbO and HbT are quite similar. 12 patients (38%) showed a positive HbO concentration change as well as a positive HbT concentration change as expected in the focus region. For 6 patients (21% of 29 patients, 50% of 12 patients), the positive concentration change in the focus region was the most significant positive change. Thus the total sensitivity and specificity based on HbO was estimated to be 38% and 21% respectively.

1.B. *Mesial temporal lobe epilepsies*

EEG-fNIRS was insensitive for 5 out of 6 patients (#6, #9, #14, #18 and #32) who suffered from MTLE, while for one patient (#20), it showed increases in HbO and in HbT in the overlying temporal neocortex albeit less significant when compared with other activations, see Appendix B.

2. Overall concordance between EEG-fNIRS response and epileptic focus region

Combing the results for neocortical epilepsy and for MTLE, we noted that, in the total 35 patients with sufficient IEDs, concordant negative HbR concentration changes could be located near the focus region in 18 patients (12 patients for HbO/HbT), wherein the changes near the focus region was the most significant in 8 patients (6 patients for HbO/HbT). As a result, the estimated HbR sensitivity dropped to 51% (34% for HbO/HbT) while the estimated HbR specificity dropped to 23% (17% for HbO/HbT), when the patient set was undifferentiated to epilepsy types.

Discussion

With the accelerated technical and methodological developments seen over the last few years, simultaneous EEG-fNIRS is getting closer to the clinical realm. In particular, our group has been working towards implementing long-term EEG-fNIRS in the epilepsy unit and neurological intensive care unit with the development of wireless and wearable multichannel wearable system dedicated for simultaneous EEG-fNIRS acquisitions at the bedside (Lareau et al., 2011; Sawan et al., 2013; Le Lan et al., 2013) and showed that the technique has definite potential to detect, localize and assess the impact of focal seizures (Nguyen et al., 2012, 2013; Pouliot et al., 2013). Although only a few patients experienced seizures during the one or two hour-long EEG-fNIRS recordings, most had IEDs on EEG. Hence, we decided to determine if such events could provide useful information. Compared with previous work (Machado et al., 2011; Pouliot et al., 2012), this study benefited from several improvements. First, a relatively large number of patients were recorded. Second, hemodynamic responses were systematically analyzed with the same processing pipeline applied to all patients. This uniformity and large sample size allowed for the first time a preliminary estimation of the sensitivity and specificity. Finally, typically about one hundred fNIRS channels provided for a large spatial coverage, which has motivated the discussion below of the concurrent hemodynamic behavior due to IEDs in other remote regions.

Sensitivity and Specificity estimates

In 18 of 29 patients with neocortical epilepsies, concordant HbR decreases due to IEDs in the epileptic focus region were observed (11 for HbO/HbT), which led to an estimation of overall sensitivity to be 62% for HbR (34% for both HbO and HbT). In 8 patients, concordant HbR decreases in the focus region were the most significant (6 for HbO/HbT), thus the overall specificity of EEG-fNIRS was estimated to be 28% for HbR (23% for HbO/HbT). Previous work from our group with fNIRS-EEG showed that temporal and frontal lobe seizures were associated with significant local hemodynamic changes resulting in a considerable sensitivity on the observation of seizures and good specificity (Nguyen et al., 2012, 2013). In this work focussing on IEDs, EEG-fNIRS showed only modest sensitivity, in part explained by the fact that IEDs evoke a less important neurovascular response compared to seizures, even when many IEDs are statistically pooled. Similar studies on the estimation of sensitivity and specificity have also been conducted with EEG-fMRI. The first assessment was done by Salek-Haddadi et al. (2006), where the authors stated that EEG-fMRI was sensitive to the hemodynamic correlates of IEDs in over 68% of their 34 patients with focal epilepsy (while no information about specificity was revealed). In a more recent EEG-fMRI study of 33 patients (Pittau et al., 2012), the estimates were much higher: the BOLD response was concordant in 29 patients (88% sensitivity) and contributed to the localization of focus in 21 patients (64% specificity). This is somewhat not surprising since EEG-fMRI has better spatial resolution, being able to assess hemodynamic changes from deep-seated structures as well, without surface physiology confounds. As expected, the EEG-fNIRS approach encountered difficulties with MTLE cases. Even if temporal IEDs detected on scalp EEG meant that IEDs from mesial structures had projected to ~ 6-10 cm^2 of

temporal neocortex (Cooper et al., 1965; Tao et al., 2007), we did not detect significant and specific temporal neocortical activations in most cases.

In real clinical practice, lateralization to the left or right hemisphere is seldom an issue as clinical manifestations and scalp EEG findings can usually provide that information. Obtaining more precise localization information within that hemisphere is the more clinically relevant need. If we had restricted our analysis only to fNIRS activations that are topographically related on the basis of observed epileptiform activity (i.e. in the assumed hemisphere of epileptogenicity), specificity would have been increased to 45% for HbR (see Table.2, column SPEC 'L') and 24% for HbO (see Appendix A) while keeping the same sensitivity (62%/38% for HbR/HbO). In this paper, we opted to remain as unbiased as possible and reported sensitivity and specificity estimates without prior assumptions on focus lateralization.

Remote hemodynamic responses

It is increasingly recognized that focal IEDs or seizures generate various hemodynamic changes in areas contiguous, contralateral or remote from the epileptic focus, observable on EEG-fNIRS, EEG-fMRI and SPECT studies (Lee et al., 2000; Huberfeld et al., 2006; Kobayashi et al., 2006; Zijlmans et al., 2011; Nguyen et al., 2012, 2013). This EEG-fNIRS study of IEDs was no different: in the 18 patients who already had significant HbR responses near the focus, similar HbR activations in the corresponding area of the contralateral lobe, were seen in 11 patients (61%, see Table.2; 50% for HbO/HbT, see Appendices A and B). More work is necessary to better understand the pathophysiology of these remote changes temporally synchronized with the IEDs.

Limitations

Due to the interpretation of fNIRS responses as cortical activations being confounded in several ways, it was recognized that the development of proper statistical method of fNIRS data was challenging. The group of Ye et al. (2009) refined the statistical threshold calculation by using the expected Euler characteristic, which can be applied at the session or at the group level (Li et al., 2012). In the present work, the EC correction at the session-level was applied (results not shown) leading to clinically reasonable results, but a practical way of pooling this information from all the sessions was not found. On the other hand, using the EC correction at the patient level would have led to a sensitivity of only 3% and no specificity at all for both HbR and HbO. Thus we observed that, when there are a small number of sessions, EC correction is not a suitable threshold to apply at the patient level, and instead a 2D-pFDR criterion was devised. In future work, pooling the sessions together in the 1st-level analysis and applying the EC correction on that will be considered, ideally by using continuous recordings.

One particular drawback in evoked brain activity detection as mentioned above is the ability to distinguish NIRS signals from various sources of noise originating from tissue layers over the brain and systemic physiology. Here a PCA was used on raw data as a filter to eliminate movement artifacts and other large fluctuations common to most channels, while a heart rate

regressor was included in the GLM to remove the effects of cardiac oscillation. Tests were conducted on the data from several patients to ensure that removing the one component with the most variance was a reasonable and effective choice to remove artefacts. A potential consequence of these filtering efforts is that the true sensitivity and specificity could have been misestimated. Improvements on this technique include the use of short source-detector separation (Zhang et al., 2007; Gagnon et al., 2011). However, due to the constraint of maintaining high spatial coverage and of instrumental gain limitations, short channels were not feasible in this study, but were considered to be included in future work.

Also, there was no standard definition to rely upon for sensitivity and specificity of EEG-fNIRS in the analysis of responses due to epileptic events. It was therefore necessary to make a practical proposal for their definition. It is possible that the reliance on experienced neurologists introduced a bias in the estimates of sensitivity and specificity in this study.

Conclusion

In this work, we extended recent developments using EEG-fNIRS in epilepsy research, contributing new evidence that this technique can detect and characterize local and remote hemodynamic changes associated with IEDs. Our preliminary observations suggest modest sensitivity and specificity to localize the epileptic focus, attributed to an inability to observe hemodynamic changes in deep seated structures and 'unexpected' large-scale effects of IEDs that are traditionally considered focal based on EEG readings. Further methodological work and validation work are clearly necessary before the move from bench to bedside.

Acknowledgements

This work was supported by the Fonds de Recherche en Santé du Québec (FRSQ) grant 14385, the Canadian Institutes of Health Research (CIHR), Institute of Circulatory and Respiratory Health (ICRH) and the Heart and Stroke Foundation of Canada (HSFC) grant 62573, and the Savoy Foundation.

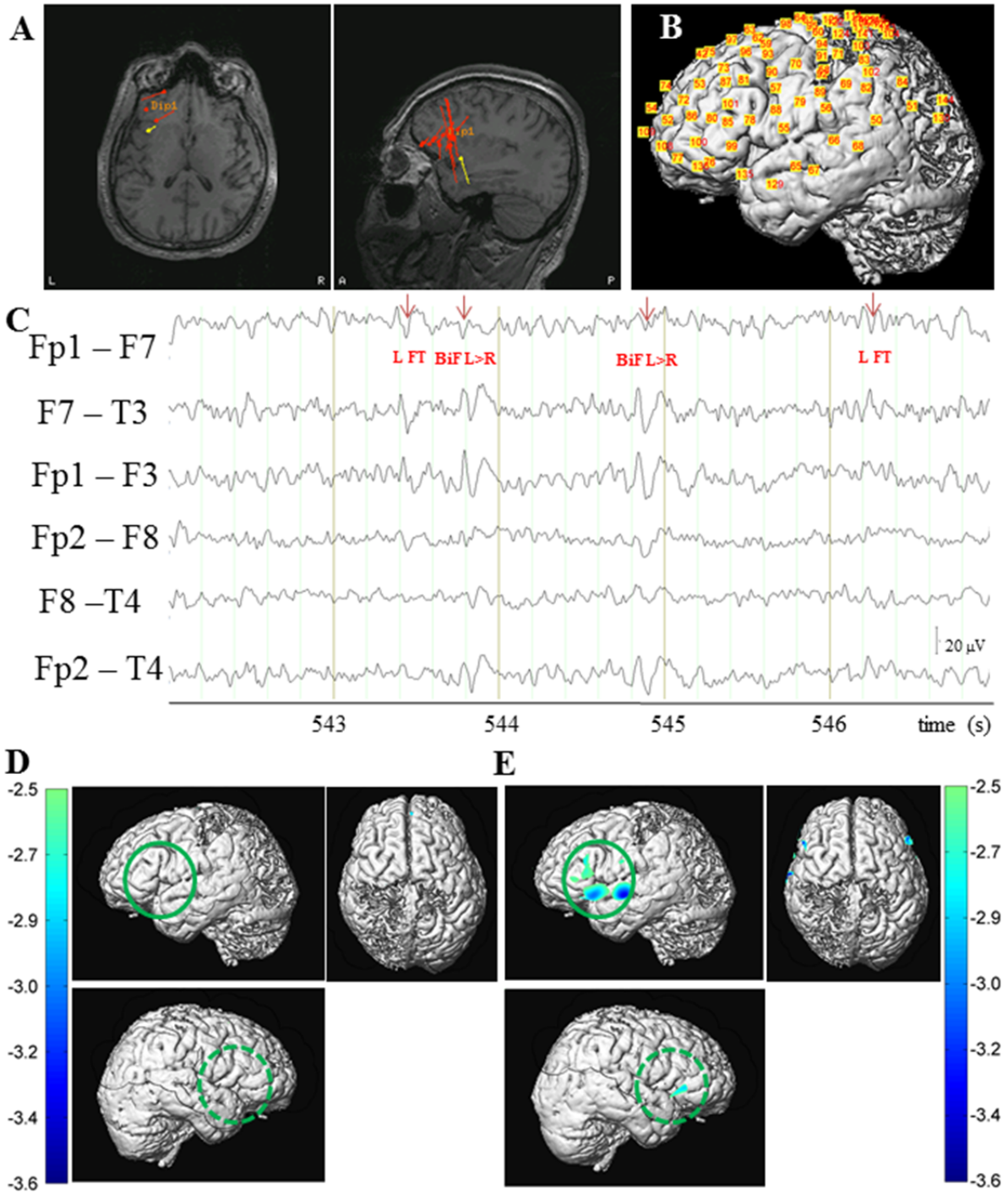

Fig.1 Patient #36. (A) MEG dipole localization of epileptic spikes revealing a cluster of sources in the L inferior frontal gyrus and L anterior insula. (B) Reconstructed NIRS channel map over grey matter layer (Left view). (C) EEG fragment with marking for L fronto-temporal and bi-frontal IEDs. (D) Hemodynamic response (HbR) to R fronto-temporal IEDs (Type I) at patient-level (2D-pFDR corrected, $p<0.05$). Solid green circle (30mm radius): focus region; dashed green circle: contralateral region corresponding to focus. (E) HbR response to bi-frontal IEDs (Type II).

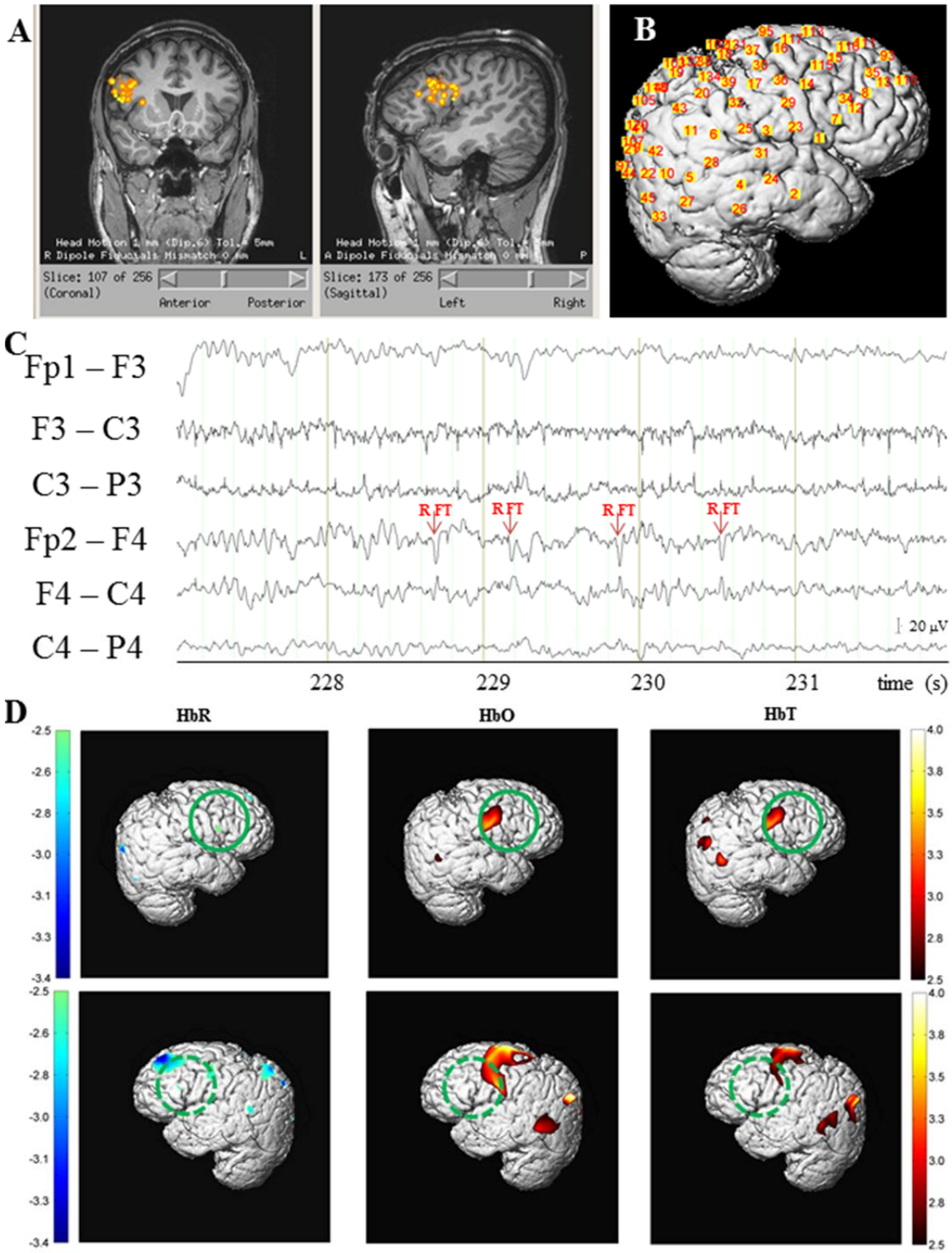

Fig.2 Patient #7. (A) MEG dipole localization of epileptic spikes revealing a cluster of sources in the right inferior frontal gyrus. (B) Reconstructed NIRS channel map over grey matter layer (Right view). (C) EEG fragment with marking for right fronto-temporal IEDs. (D) Hemodynamic responses to right fronto-temporal IEDs, patient level (2D-pFDR corrected, $p<0.05$). Solid green circle (30mm radius): focus region; dotted green circle: contralateral region corresponding to focus.

Table.1 Types and total numbers of IEDs identified on EEG recordings

Neocortical Epilepsy

#	Focus	IED Type (Number)	Number of Channels	Number of Sessions	Recording Time(min)	#	Focus	IED Type (Number)	Number of Channels	Number of Sessions	Recording Time(min)
1	R F(polar)	R F (105)	28	5	81	**24**	R F(IFG)	R FC (298)	135	4	60
2	R P	R P (605)	49	2	35	**25**	L F(SFG+MFG)	L FC (1023)	203	7	100
3	L F(SFG+MFG)	L (865)	45	5	76	**26**	L T(PostMTG+ITG)	L T (1424)	152	5	72
4	L F(MFG)	L CP (3283)	53	7	102	**27**	R T	R T (1128), L T (138)	144	6	87
5	L T(PostSTG+MTG)	L T (72)	57	2	19	**28**	L OrbitalF, L F(IFG)	L T (1969), L F (279)	132	8	120
7	R F(IFG)	R FT (2302) biD R>L (6) biF R>L (15)	134	4	54	**29**	R F(IFG)	R F (1541)	92	4	60
8	R F(IFG+MFG)	R F (238)	94	8	129	**30**	L O	L TO (1157)	107	3	45
10	R F(IFG) R INS	biF R>L (1317), biF L>R (524) F (115)	73	7	100	**31**	R OrbitalF, RF aINS	R FT (494)	129	4	60
11	L T(STG), L INS L F(IFG)	L T (305)	127	7	107	**33**	R F(IFG), R aINS	R F (103)	142	7	106
12	L T(STG) L F(IFG), L INS	L (16)	135	1	15	**35**	R T(PostMTG+ITG) L T	R T (389) L T (23)	146	6	90
13	L T(PostMTG+STG)	L T (97) L F (153)	146	12	181	**36**	L aINS, L F(IFG)	L FT (1088), L F (5) BiF L>R (1450)	144	4	50
15	R INS	R T (63)	106	6	84	**38**	R T(PostITG), R O	R T (666), R FT (530)	106	6	83
16	R F(SFG), R PreCG	R C (3377)	174	3	47	**39**	R F(SFG), R SMA	Cz (550)	121	5	70
21	R F(IFG)	R F (781)	141	6	83	**40**	L PreCG	L F (117)	140	9	135
23	L F(SFG+MFG)	L FCP (1210)	118	5	38						

Mesial Temporal Lobe Epilepsy

#	Focus	IED Type (Number)	Number of Channels	Number of Sessions	Recording Time(min)	#	Focus	IED Type (Number)	Number of Channels	Number of Sessions	Recording Time(min)
6	L T(mesial) R T(mesial)	L T (242) R T (577)	68	3	41	**18**	L T(mesial)	L F (74), L T (44)	133	6	83
9	R T(mesial)	R T (148), R FT (34)	61	6	90	**20**	L T(mesial)	L FT (159)	153	10	143
14	R T(mesial) L T(mesial)	R T (43) L T (1148)	150	11	156	**32**	L T(mesial)	L T (249), L CP (6)	101	5	74

Abbreviations: L: Left; R: Right; F: Frontal; T: Temporal; P: Parietal; O: Occipital; C: Center; SFG: Superior frontal gyrus; MFG: Middle frontal gyrus; IFG: Inferior frontal gyrus; CG: Central gyrus; STG: Superior temporal gyrus; MTG: Middle temporal gyrus; ITG: Inferior temporal gyrus; Post: Posterior; INS: Insular; aINS: anterior insular; SMA: Supplementary motor area.

Table.2 Hemodynamic response regions of focal IEDs in neocortical epilepsy (HbR)

Neocortical Epilepsy										
#	Focus	Hemodynamic response					SENS	SPEC		MIRR
		Congruent with focus	Outside focus				↓	U	L	
			Intra lobar	Extra lobar	Contralateral					
					Mirrored (to focus)	Not-Mirrored				
1	RF(polar)	↓↓R F (polar)					1	1	1	0
2	RP						0	0	0	
3	L F (SFG+MFG)				↓↓R F (SFG+MFG)		0	0	0	
4	L F(MFG)	↓↓L F (MFG)					1	1	1	0
5	L T (postSTG +MTG)						0	0	0	
7	R F (IFG)	↓R F (IFG)		↓RO	↓L F (IFG)	↓↓L F (SFG), ↓L T, ↓L P	1	0	0	1
8	R F (IFG+MFG)	↓R F (IFG)				↓↓L P	1	0	1	0
10	R F (IFG), R INS		↓↓R F (SFG)	↓R F (PreCG)	↓L F (IFG)	↓LT (STG)	0	0	0	
11	L T(STG) L F (IFG), L INS		↓L F (SFG)		↓L F (IFG)	↓↓R F (preCG)	0	0	0	
12	L T (STG) L F (IFG) L INS						0	0	0	0
13	L T (postMTG + STG)	↓L T (postMTG)		↓L F (IFG)	↓R F (postCG)	↓↓R F (SFG + postCG)	1	0	0	1
15	R INS						0	0	0	
16	R PreCG R F (SFG)						0	0	0	
21	R F (IFG)	↓R F (IFG)	↓R preCG ↓R F(SFG)	↓R T (STG)	↓↓L F (IFG)	↓L T (STG)	1	0	1	1
23	L F (SFG+MFG)	↓L F (SFG)			↓R F (SFG)	↓↓R T (Post STG) ↓R F (MFG)	1	0	1	1
24	R F (IFG)						0	0	0	
25	L F (SFG + MFG)	↓↓L F (SFG + MFG)	↓L F (IFG)		↓R F (SFG+MFG)		1	1	1	1
26	L T (PostMTG + ITG)	↓↓L PostMid	↓L T (STG)				1	1	1	0
27	R T					↓↓L F (IFG)	0	0	0	
28	L ObitalF L F (IFG)			↓↓L P		↓R F (SFG)	0	0	0	
29	R F (IFG)	↓R F (IFG)			↓L F (IFG)	↓↓L T (PostTG)	1	0	1	1
30	L O	↓↓L O				↓R P	1	1	1	0
31	R aINS, R F(IFG)	↓R F (IFG)			↓L F (IFG)	↓L T (ITG) ↓↓L F (SFG)	1	0	1	1
33	R F (IFG), R aINS	↓R F (IFG)		↓↓R P			1	0	0	0
35	RT (PostMTG+ITG)	↓R T (STG)	↓R T (STG)		↓L T	↓L P, ↓↓L F (IFG)	1	0	0	1
36	L aINS, L F (IFG)	↓↓L F (IFG)		↓L T (STG)	↓R F (IFG)		1	1	1	1
38	R postITG,R O	↓R T, ↓R O		↓R P	↓↓L P	↓L T, ↓L O	1	0	0	1
39	R F (SFG), R SMA	↓R F (SFG) ↓↓R SMA					1	1	1	0
40	L PreCG	↓↓L PreCG			↓R PreCG		1	1	1	1
					Neocortical Epilepsy Subtotal (Percentage, 29 subjects in total)		62	28	45	61

Abbreviations: L: Left; R: Right; F: Frontal; T: Temporal; P: Parietal; O: Occipital; C: Center; SFG: Superior frontal gyrus; MFG: Middle frontal gyrus; IFG: Inferior frontal gyrus; CG: Central gyrus; STG: Superior temporal gyrus; MTG: Middle temporal gyrus; ITG: Inferior temporal gyrus; Post: Posterior; INS: Insular; aINS: anterior insular; SMA: Supplementary motor area; SENS: sensitivity; SPEC: specificity; U: unbiased; L: pre-lateralized; MIRR: mirrored activation.

Appendix A. Hemodynamic response regions of focal IEDs in neocortical epilepsy (HbO/HbT)

Neocortical Epilepsy

#	Focus	Hemodynamic response					SENS	SPEC		MIRR
		Congruent with focus	Outside focus				↑	U	L	
			Intra lobar	Extra lobar	Contralateral					
					Mirrored (to focus)	Not-Mirrored				
1	RF(polar)		↑↑R PreCG (HbT)				0	0	0	
2	RP						0	0	0	
3	L F (SFG+MFG)	↑↑L F (SFG)			↑R F (SFG) (HbT)		1	1	1	0/1
4	L F(MFG)	↑↑L F (SFG)			↑R PreCG (HbO)		1	1	1	1/0
5	L T (postSTG+MTG)						0	0	0	
7	R F (IFG)	↑R F (IFG)			↑L F (IFG)	↑↑L F (SFG), ↑L T, ↑L P	1	0	1	1
8	R F (IFG+MFG)				↑↑L F (IFG) (HbO) ↑L F (IFG) (HbT)	↑L P (HbO) ↑↑L F (PosCG) (HbT)	0	0	0	
10	R F (IFG) R INS	↑R F (IFG)	↑R F (MFG+SFG)	↑R T (PosITG) (HbO)	↑↑L F (IFG+MFG)	↑L (PreCG)	1	0	0	1
11	L T(STG) L F (IFG) L INS	↑↑L F (IFG)			↑R F (IFG)	↑R P (HbT)	1	1	1	1
12	L T (STG) L F (IFG) L INS						0	0	0	
13	L T (postMTG + STG)	↑↑L T (PostSTG)			↑R T (STG)		1	1	1	1
15	R INS						0	0	0	
16	R PreCG R F (SFG)						0	0	0	
21	R F (IFG)	↑↑R F (IFG)	↑R F (SFG)			↑L T (MTG) (HbO)	1	1	1	0
23	L F (SFG+MFG)			↑L T (STG + MTG) (HbO) ↑L T (STG) (HbT)		↑↑R T (STG + MTG)	0	0	0	
24	R F (IFG)						0	0	0	
25	L F (SFG + MFG)			↑↑L P			0	0	0	
26	L T (PostMTG + ITG)	↑L T (MTG + ITG)		↑↑L P, ↑L O		↑R P	1	0	0	0
27	R T	↑R T (MTG)		↑↑R O, ↑R P		↑L P	1	0	0	0
28	L ObitalF L F (IFG)					↑↑RPostCG	0	0	0	
29	R F (IFG)	↑R F (MFG)	↑R F (MFG) (HbO) ↑↑R F (MFG) (HbT)	↑R P ↑R postCG		↑↑L PreCG (HbO) ↑L PreCG (HbT) ↑L F	1	0	0	0
30	L O					↑↑R P (HbO)	0	0	0	
31	R aINS, R orbtoF (IFG)					↑↑L F (polar) (HbT)	0	0	0	
33	R F (IFG) R aINS					↑↑L T (MTG)	0	0	0	
35	R T (postMTG + ITG)		↑↑R PreCG			↑L F (MFG)	0	0	0	
36	L aINS ,L F (IFG)						0	0	0	
38	R postITG, R O			↑R O, ↑R P		↑↑L O	0	0	0	
39	RF (SFG) R SMA		↑R F (IFG) (HbT)		↑↑L F (SFG)		0	0	0	
40	L PreCG	↑↑L PreCG			↑R PreCG	↑R P	1	1	1	1
					Neocortical Epilepsy Subtotal (Percentage, 29 subjects in total)		38	21	24	55

Abbreviations: L: Left; R: Right; F: Frontal; T: Temporal; P: Parietal; O: Occipital; C: Center; SFG: Superior frontal gyrus; MFG: Middle frontal gyrus; IFG: Inferior frontal gyrus; CG: Central gyrus; STG: Superior temporal gyrus; MTG: Middle temporal gyrus; ITG: Inferior temporal gyrus; Post: Posterior; INS: Insular; aINS: anterior insular; SMA: Supplementary motor area; SENS: sensitivity; SPEC: specificity; U: unbiased; L: pre-lateralized; MIRR: mirrored activation.

Appendix B. Hemodynamic response regions of focal IEDs in mesial temporal lobe epilepsy (HbR/HbO/HbT)

Mesial Temporal Lobe Epilepsy

#	Focus	Hemodynamic response					SENS	SPEC		MIRR
		Congruent with focus	Outside focus					U	L	
			Intra lobar	Extra lobar	Contralateral					
					Mirrored (to focus)	Not-Mirrored				
HbR										
	L T (mesial)						0	0	0	
6	R T (mesial)						0	0	0	
9	R T (mesial)			↓↓R F (MFG)		↓L F (MFG)	0	0	0	
	R T (mesial)			↓R F (SFG)		↓↓L F (MFG +SFG)	0	0	0	
14	L T (mesial)					↓↓R F (SFG)	0	0	0	
18	L T (mesial)			↓L P		↓↓R T (PostMTG) ↓R inf P	0	0	0	
20	L T (mesial)			↓LF (MFG)		↓↓R F (MFG)	0	0	0	
32	L T (mesial)		↓L postT	↓↓L preCG ↓L postCG		↓R preCG ↓R postCG	0	0	0	
						HbR: MTLE Subtotal (Percentage, 6 subjects in total)	0	0	0	
						HbR: Overall (Neocortical epilepsy + MTLE Percentage, 35 subjects in total)	51	23	37	61
HbO/HbT										
	L T (mesial)						0	0	0	
6	R T (mesial)			↑↑R F (IFG) (HbT)			0	0	0	
9	R T (mesial)					↑↑L F (IFG)	0	0	0	
	R T (mesial)			↑R PreCG ↑R F (IFG)		↑↑L F (IFG+ MFG)	0	0	0	
14	L T (mesial)			↑↑L F (SFG)		↑R F (IFG)	0	0	0	
18	L T (mesial)			↑L PreCG		↑↑R T (ITG)	0	0	0	
20	L T (mesial)	↑L T (antiMTG)	↑L T (MTG)	↑↑L F (IFG)			1	0	0	0
32	L T (mesial)			↑L Post CG ↑L P ↑↑L PreCG (HbO)		↑R PreCG (HbO) ↑R PostCG (HbO) ↑↑R P (HbT)	0	0	0	
						HbO/HbT: MTLE Subtotal (Percentage, 6 subjects in total)	17	0	0	
						HbO/HbT: Overall (Neocortical epilepsy + MTLE Percentage, 35 subjects in total)	34	17	20	50

Abbreviations: L: Left; R: Right; F: Frontal; T: Temporal; P: Parietal; O: Occipital; C: Center; SFG: Superior frontal gyrus; MFG: Middle frontal gyrus; IFG: Inferior frontal gyrus; CG: Central gyrus; STG: Superior temporal gyrus; MTG: Middle temporal gyrus; ITG: Inferior temporal gyrus; Post: Posterior; INS: Insular; aINS: anterior insular; SMA: Supplementary motor area; SENS: sensitivity; SPEC: specificity; U: unbiased; L: pre-lateralized; MIRR: mirrored activation.

References

Benjamini, Y., Hochberg, Y., 1995. Controlling the false discovery rate: a practical and powerful approach to multiple testing. Journal of the Royal Statistical Society. Series B. Methodological 57, 289–300.

Chumbley, J., Worsley, K., Flandin, G., Friston, K., 2010. Topological FDR for neuroimaging. Neuroimage 49, 3057–3064.

Cooper, R., Winter, A.., Crow, H.., Walter, W.G., 1965. Comparison of subcortical, cortical and scalp activity using chronically indwelling electrodes in man. Electroencephalography and Clinical Neurophysiology 18, 217–228.

Delpy, D.T., Cope, M., 1997. Quantification in tissue near-infrared spectroscopy. Philos Trans R Soc Lond B Biol Sci 352, 649–659.

Desjardins, M., Pouliot, P., Lesage, F., 2012. Principles and Applications of Diffuse Optical Imaging for the Brain. Current Medical Imaging Reviews 8, 157–173.

Friston, K.J., Ashburner, J.T., Kiebel, S.J., Nichols, T.E., Penny, W.D., 2007. Statistical Parametric Mapping: The Analysis of Functional Brain Images. Academic Press.

Friston, K.J., Fletcher, P., Josephs, O., Holmes, A., Rugg, M.D., Turner, R., 1998. Event-related fMRI: characterizing differential responses. Neuroimage 7, 30–40.

Gagnon, L., Perdue, K., Greve, D.N., Goldenholz, D., Kaskhedikar, G., Boas, D.A., 2011. Improved recovery of the hemodynamic response in diffuse optical imaging using short optode separations and state-space modeling. NeuroImage 56, 1362–1371.

Geneslaw, A.S., Zhao, M., Ma, H., Schwartz, T.H., 2011. Tissue hypoxia correlates with intensity of interictal spikes. Journal of Cerebral Blood Flow and Metabolism 31, 1394–402.

Gotman, J., 2008. Epileptic networks studied with EEG-fMRI. Epilepsia 49 Suppl 3, 42–51.

Gotman, J., Kobayashi, E., Bagshaw, A.P., Bénar, C.-G., Dubeau, F., 2006. Combining EEG and fMRI: a multimodal tool for epilepsy research. J Magn Reson Imaging 23, 906–920.

Huberfeld, G., Habert, M.-O., Clemenceau, S., Maksud, P., Baulac, M., Adam, C., 2006. Ictal Brain Hyperperfusion Contralateral to Seizure Onset: The SPECT Mirror Image. Epilepsia 47, 123–133.

Irani, F., Platek, S.M., Bunce, S., Ruocco, A.C., Chute, D., 2007. Functional near infrared spectroscopy (fNIRS): an emerging neuroimaging technology with important applications for the study of brain disorders. Clin Neuropsychol 21, 9–37.

Jang, K.E., Tak, S., Jung, J., Jang, J., Jeong, Y., Ye, J.C., 2009. Wavelet minimum description length detrending for near-infrared spectroscopy. J Biomed Opt 14, 034004.

Jöbsis, F.F., 1977. Noninvasive, infrared monitoring of cerebral and myocardial oxygen sufficiency and circulatory parameters. Science 198, 1264–1267.

Kobayashi, E., Bagshaw, A.P., Benar, C.-G., Aghakhani, Y., Andermann, F., Dubeau, F., Gotman, J., 2006. Temporal and Extratemporal BOLD Responses to Temporal Lobe Interictal Spikes. Epilepsia 47, 343–354.

Lareau, E., Lesage, F., Pouliot, P., Nguyen, D., Le Lan, J., Sawan, M., 2011. Multichannel wearable system dedicated for simultaneous electroencephalography/near-infrared spectroscopy real-time data acquisitions. J. Biomed. Opt 16, 096014–096014.

Le Lan, J., Dupuy, O., Kassab, A., Dehbozorgi, M., Pouliot, P., Vannasing, P., Nguyen, D.K., Fraser, S.A., Bherer, L., Lassonde, M., Lesage, F., Sawan, M., 2013. High-Channel-Count Wearable NIRS-EEG System for Long-Term Clinical Imaging. submitted to Journal of Biomedical Optics.

Lee, S.K., Lee, S.H., Kim, S.K., Lee, D.S., Kim, H., 2000. The clinical usefulness of ictal SPECT in temporal lobe epilepsy: the lateralization of seizure focus and correlation with EEG. Epilepsia 41, 955–962.

Li, H., Tak, S., Ye, J.C., 2012. Lipschitz-Killing curvature based expected Euler characteristics for p-value correction in fNIRS. Journal of Neuroscience Methods 204, 61–67.

Lloyd-Fox, S., Blasi, A., Elwell, C.E., 2010. Illuminating the developing brain: The past, present and future of functional near infrared spectroscopy. Neuroscience & Biobehavioral Reviews 34, 269–284.

Machado, A., Lina, J.M., Tremblay, J., Lassonde, M., Nguyen, D.K., Lesage, F., Grova, C., 2011. Detection of hemodynamic responses to epileptic activity using simultaneous Electro-EncephaloGraphy (EEG)/Near Infra Red Spectroscopy (NIRS) acquisitions. Neuroimage 56, 114–125.

Nguyen, D.K., Tremblay, J., Pouliot, P., Vannasing, P., Florea, O., Carmant, L., Lepore, F., Sawan, M., Lesage, F., Lassonde, M., 2012. Non-invasive continuous EEG-fNIRS recording of temporal lobe seizures. Epilepsy Research 99, 112–126.

Nguyen, D.K., Tremblay, J., Pouliot, P., Vannasing, P., Florea, O., Carmant, L., Lepore, F., Sawan, M., Lesage, F., Lassonde, M., 2013. Noninvasive continuous functional near-infrared spectroscopy combined with electroencephalography recording of frontal lobe seizures. Epilepsia 54, 331–340.

Penfield, W., Jasper, H., 1954. Epileptic Mechanisms (cortical circulation), in: Epilepsy and the Functional Anatomy of the Human Brain. Little, Brown and Company Ed., Boston, pp. 246–264.

Pittau, F., Dubeau, F., Gotman, J., 2012. Contribution of EEG/fMRI to the definition of the epileptic focus. Neurology 78, 1479–1487.

Pouliot, P., Tran, T.P.Y., Birca, V., Vannasing, P., Tremblay, J., Lassonde, M., Nguyen, D.K., 2013. Hemodynamic changes during posterior epilepsies: an EEG-fNIRS study. Submitted to Epilepsy Research.

Pouliot, P., Tremblay, J., Robert, M., Vannasing, P., Lepore, F., Lassonde, M., Sawan, M., Nguyen, D.K., Lesage, F., 2012. Nonlinear hemodynamic responses in human epilepsy: A multimodal analysis with fNIRS-EEG and fMRI-EEG. Journal of Neuroscience Methods 204, 326–340.

Saito, S., Yoshikawa, D., Nishihara, F., Morita, T., Kitani, Y., Amaya, T., Fujita, T., 1995. The cerebral hemodynamic response to electrically induced seizures in man. Brain Res. 673, 93–100.

Salek-Haddadi, A., Diehl, B., Hamandi, K., Merschhemke, M., Liston, A., Friston, K., Duncan, J.S., Fish, D.R., Lemieux, L., 2006. Hemodynamic correlates of epileptiform discharges: an EEG-fMRI study of 63 patients with focal epilepsy. Brain Res. 1088, 148–166.

Sawan, M., Salam, M.T., Le Lan, J., Kassab, A., Gelinas, S., Vannasing, P., Lesage, F., Lassonde, M., Nguyen, D.K., 2013. Wireless Recording Systems: From Noninvasive EEG-NIRS to Invasive EEG Devices. IEEE Transactions on Biomedical Circuits and Systems 7, 186–195.

Staley, K.J., Dudek, F.E., 2006. Interictal Spikes and Epileptogenesis. Epilepsy Curr 6, 199–202.

Suh, M., Ma, H., Zhao, M., Sharif, S., Schwartz, T.H., 2006. Neurovascular coupling and oximetry during epileptic events. Mol. Neurobiol. 33, 181–197.

Tao, J.X., Baldwin, M., Hawes-Ebersole, S., Ebersole, J.S., 2007. Cortical substrates of scalp EEG epileptiform discharges. J Clin Neurophysiol 24, 96–100.

Ye, J.C., Tak, S., Jang, K.E., Jung, J., Jang, J., 2009. NIRS-SPM: Statistical parametric mapping for near-infrared spectroscopy. NeuroImage 44, 428–447.

Zhang, Q., Brown, E.N., Strangman, G.E., 2007. Adaptive filtering for global interference cancellation and real-time recovery of evoked brain activity: A Monte Carlo simulation study. Journal of Biomedical Optics 12.

Zijlmans, M., Jacobs, J., Kahn, Y.U., Zelmann, R., Dubeau, F., Gotman, J., 2011. Ictal and interictal high frequency oscillations in patients with focal epilepsy. Clin Neurophysiol 122, 664–671.